Article

Corrosion Inhibition Using Harmal Leaf Extract as an Eco-Friendly Corrosion Inhibitor

Nasreen Al Otaibi * and Hassan H. Hammud *

Department of Chemistry, College of Science, King Faisal University, P.O. Box 400, Al-Ahsa 31982, Saudi Arabia
* Correspondence: nbalotaibi@kfu.edu.sa (N.A.O.); hhammud@kfu.edu.sa (H.H.H.)

Abstract: Extract of natural plants is one of the most important metallic corrosion inhibitors. They are readily available, nontoxic, environmentally friendly, biodegradable, highly efficient, and renewable. The present project focuses on the corrosion inhibition effects of Peganum Harmala leaf extract. The equivalent circuit with two time constants with film and charge transfer components gave the best fitting of impedance data. Extraction of active species by sonication proved to be an effective new method to extract the inhibitors. High percent inhibition efficacy IE% of 98% for 283.4 ppm solutions was attained using impedance spectroscopy EIS measurements. The values of charge transfer R_{ct} increases while the double layer capacitance C_{dl} values decrease with increasing Harmal extract concentration. This indicates the formation of protective film. The polarization curves show that the Harmal extract acts as a cathodic-type inhibitor. It is found that the adsorption of Harmal molecules onto the steel surface followed Langmuir isotherm. Fourier-transform infrared spectroscopy FTIR was used to determine the electron-rich functional groups in Harmal extract, which contribute to corrosion inhibition effect. Scanning electron microscopy SEM measurement of a steel surface clearly proves the anticorrosion effect of Harmal leaves.

Keywords: Harmal leaves; anticorrosion; equivalent electrical circuit; EIS; Tafel

1. Introduction

Inhibition of corrosion of metals represents a major challenge in the industry. The main concern is to retard the extensive corrosion of different parts of oil production plants, tubing, and pipelines from the wellhead equipments. Corrosion is caused by the contact of metal surface with dissolved carbon dioxide, hydrogen sulfide, as well as salts [1]. Metallic corrosion causes huge yearly losses in the United States [2]. Inhibition of corrosion by adsorption inhibitors has been applied in different technologies such as acid pickling and descaling, petrochemicals, and storage of chemicals [3,4].

Many inorganic compounds such as chromium and manganese organic complexes were used as corrosion inhibitors in different media [5–9]. These low cost complexes were able to decrease efficiently the corrosion of different metals, such as Fe, Al, and Cu [9,10]. However, their use as corrosion inhibitors leads to environmental pollution. This makes them less applicable [10,11].

The world becomes much aware of the environmental problems and the toxic effects of the used chemicals in different industries. Nowadays there is growing attention towards eco-friendly corrosion inhibitions "green corrosion inhibitors". There are several advantages of these naturally obtained inhibitors. They are readily available, environmentally friendly, biodegradable, efficient, and renewable [12–16].

Those eco-friendly inhibitors can be easily extracted from plants. The next important step is to separate, identify different species, and correlate them to the inhibition effectiveness. Moreover, the study of the inhibition effects of the extracted species alone or in combination was carried out to investigate the possibility of synergism or antagonism that ensures an optimum level of inhibition [17–21]. The organic extracts from plant leaves,

barks, seeds, fruits, and roots act as green corrosion inhibitors in different aggressive media. The extracts containing nitrogen, sulfur and oxygen functional groups exhibit good inhibition. Because, these groups having free electrons can bind to partially dissolved metal ions, retarding further dissolution and corrosion [22–25].

Recently several ecofriendly corrosion inhibitors were studied. Corrosion of mild steel in HCl solution was investigated using extracts of leaves as green inhibitors: the extract of Salvia leaves acted as anticorrosion on stainless steel using polarization studies. The efficiency was due to the presence of phenolic components [26]. The inhibition of carbon steel corrosion was investigated using Phyllanthus amarus leaf extract [27]. The adsorption of plant extract followed Langmuir isotherm. Also, polarization curves indicated that the plant extract act as an anodic inhibitor and cathodic inhibitor. Alkaloids extract of Geissospermum leave was studied as an inhibitor for carbon C-steel corrosion using electrochemical methods, Scanning electron microscopy SEM and Energy-dispersive X-ray spectroscopy EDX [28]. The results indicated that plant extract has high inhibition efficiency IE% of 92%. Also, Acalypha torta leaves extracts were used to inhibit corrosion of mild steel. Weight loss, electrochemical procedure, and UV-Visible spectroscopy was used to assess the inhibition efficiency. The reported inhibition efficiency was nearly 90% at 1000 ppm extract solution [29].

As well as extracts from Aloe Vera leaves were studied in 1 M H_2SO_4 solution. Electrochemical and SEM techniques were applied to study the inhibition effect of the extract on corrosion. The results indicated that plant extract acts as a mixed type inhibitor for mild steel with IE% of 98% at 30% v/v concentration [30]. Extracts of Citrus aurantium leaves have been employed as an eco-friendly corrosion inhibitor for mild steel in aqueous acid media. The results indicated that adsorption of molecular extract followed Langmuir isotherm [31].

Furthermore, many types of green corrosion inhibitors have been evidenced such as Cassia tora. They showed highly effective corrosion inhibition in NaCl media [32]. Also extract of Ricinus was studied to reduce the mild steel corrosion in aqueous solution. The extract showed IE% of 84% at 300 ppm concentration [33]. Neem and African star apple leaf extracts were used as green corrosion inhibitors for mild steel in NaCl and polluted seawater media [34,35]. The corrosion inhibition of steel in neutral chloride solution using Nicotiana leaves extract was studied using electrochemical techniques [36]. The investigated results showed that Nicotiana extract acts as a mixed type inhibitor. The effect of Ficus carica leaf extract on steel anticorrosion in petroleum solution was investigated [37]. Results indicate that the extract show percent inhibition efficiency IE% of 70–80% and act as cathodic and anodic inhibitors. The adsorption of extract caused corrosion inhibition and obeyed Langmuir isotherm model.

In the current project, we studied the corrosion inhibition of carbon steel in 0.25 M H_2SO_4 using plant Harmal extract that grows in the desert of Saudi Arabia. The constituents of Harmal extract are shown in Figure 1, [38]. Harmal leaves extract unlike other synthesized chemicals are expected to be biodegradable. They can be decomposed by bacteria or other living organisms and thereby avoiding pollution. Harmal leaves extract contains flavonoids, alkaloids, and anthraquinones. Flavonoids are beneficial to human body due to their anti-oxidant activity. Anthraquinones are antibacterial and antiviral. Alkaloids such as harmine and harmol are biologically active. They are cytotoxic to cancer cells and act as an antiviral and antioxidant. However, they are toxic at high doses, causing hallucination [38,39]. *P. harmal* has a wide range of pharmacological effects. However, there has been several reports of intoxications due to ingestion of specific quantity of *P. harmal* seeds. Thus, care should be taken by clinicians regarding usage of this plant [40].
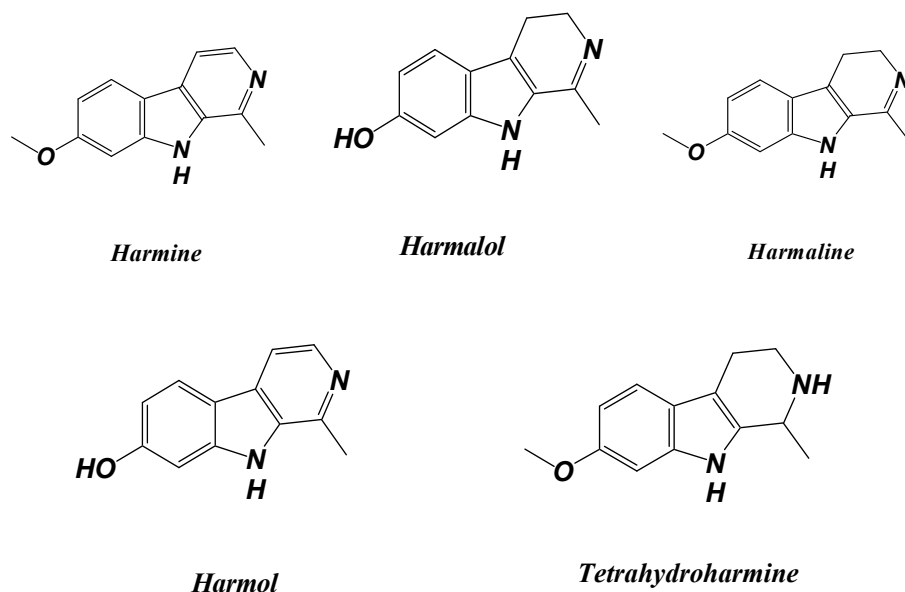
Figure 1. The chemical structure of the major constituents of Harmal extract.

This project study the use of Harmal plant extracts as green corrosion inhibitor. The extract contains electron rich nitrogen and oxygen functional group that can bind to electron poor metal ion present on the exposed metallic surface. Further study is underway to make the extract commercially viable model. This project use impedance and potentiodynamic measurement in order to determine the efficiency of inhibition. The determination of corrosion properties can be also useful in energy production [41,42].

2. Experimental

2.1. Materials

Chemicals: Ethanol absolute ($\geq$99.8%), Honeywell-France; Sulfuric acid (95–98%), Scharlau, Spain.

2.1.1. Extraction of Harmal Leaves

A new extraction method "sonication" was used in this research. This method has proven effective in shortening the time. Compared to classical method where the plant is usually soaked for up to days, and extracted by using the Soxhlet apparatus several times. This ultrasound-assisted extraction not only reduce extraction times but also extractant volumes [43].

Harmal leaves were collected from Alhasa in the east regain of Saudi Arabia. The collected leaves were dried in the shad, and then ground to powder. 100 g powder of Harmal leaves were added to 100 mL ethanol in the bottom flask, which was then continuously sonicated for 1 h at 80 kHz using a Power Sonic405. The mixture was then filtered, and dried using a rotary evaporator. 1 g of green powder was obtained (1% yield).

The prepared dried Harmal extract is readily soluble in water, methanol, and ethanol. A stock solution of 10,000 ppm Harmal extract was prepared by dissolving 250 mg extract in 25 mL deionized water. In the inhibition of C-steel experiments, aliquots from this stock solution were used to prepare diluted Harmal solutions of concentrations (0, 20.79, 41.49, 62.11, 82.65, 204.1, 283.4, 625.0 and 826.5 ppm) in H_2SO_4 (0.25 M) medium.

2.1.2. Preparation of the Specimens

The carbon steel rod with the following chemical composition % weight (wt%) C, 0.164; S, 0.001; Mn, 0.710; P, 0.0005; Si, 0.26, Ni, 0.123; Cr, 0.041; balance Fe, was used as a working electrode in electrochemical study. The exposed area of cylindrical carbon C-steel of cylindrical shape was (0.8 cm^2). The working electrode was buffed with a series

of silicon carbide papers from 600 to 1200 before the experiments. Each electrode was immersed in 0.25 M H_2SO_4 solution containing 20.79–826.50 ppm of the Harmal extract. C-steel plates with dimensions of 1 cm $\times$ 1 cm $\times$ 0.1 cm and chemical composition (wt%) of C 2.41%, Mn 0.69%, S 0.27%, (the balance was Fe) were immersed in Harmal extract solutions. The morphology of surfaces of plates was monitored by SEM microscope in order to study the effect of anticorrosion.

2.2. Methods

2.2.1. Characterization of Harmal Leaves

FTIR analysis was used to determine the most important functional groups in the dried Harmal leaves and their extract. Infrared (IR) absorption bands were recorded using Agilent Technologies Cary 630 FTIR. UV-visible spectra was recorded using Shimadzu UV-1800 UV/Visible Scanning Spectrophotometer.

2.2.2. Scanning Electron Microscopy

The surface morphology of C-steel specimens immersed for 3 h in 0.25 M H_2SO_4 or 0.25 M H_2SO_4 + Harmal extract respectively, were studied using a FEI Quanta FEC 250 Scanning electron microscopy (SEM) microscope. The specimens were immersed in the test solutions for 2 h before analysis at room temperature.

2.2.3. Electrochemical Studies

The electrochemical study was performed at room temperature. Electrochemical impedance study (EIS) and Potentiodynamic polarization study (PDP) measurements were carried out using (Gamry, reference 600 Potentiostat/Galvanostat/ZRA, Warminster, PA, USA) and Gamry software v7.07. The cell used consisted of a platinum wire auxiliary electrode (PtE), and a saturated calomel reference electrode (SCE) electrode. C-steel rod with area (0.5027 cm^2) was used as working electrode. Before the start of the experiment, the steady-state open circuit potential E_{OCP} was measured by immersing the electrode in the corrosion solution for 15 min with the indication 10 mV disturbance capacity.

2.2.4. Electrochemical Impedance Study (EIS)

EIS was measured at frequency range 0.1–100,000 Hz with a signal amplitude perturbation of 10 mV around the corrosion potential. Before the start of the experiment, the electrode is immersed in the corrosion solution with or without Harmal extract at different concentrations till reaching a steady state. The obtained impedance results were represented as Nyquist plot and Bode plot. The following Equation (1) is used to calculate the inhibition efficiency (IE%) from Nyquist plot [44].

$$\text{IE\%} = \left(1 - \frac{Rct(0)}{Rct(i)}\right) \times 100 \tag{1}$$

where $Rct(0)$ is the charge transfer resistance of C-steel without Harmal extract. $Rct(i)$ is the charge transfer resistance of C-steel with Harmal extract. Also, the surface coverage θ were calculated using Equation (2):

$$\theta = 1 - \frac{Rct(0)}{Rct(i)} \tag{2}$$

2.2.5. Potentiodynamic Polarization Study (PDP)

Measurements of polarization curves were obtained by automatically polarizing the working electrode from 500 mV versus the rest potential with a scanning rate of 5 mV/s. Corrosion current density (i_{corr}) were obtained from the extrapolation of the points to

corrosion potential Ecorr. Equation (3) below shows the calculation of IE(%) from the i_{corr} values [45].

$$IE\% = \left(1 - \frac{icorr(i)}{icorr(0)}\right) \times 100 \tag{3}$$

where $i_{corr(i)}$ and $i_{corr(0)}$ are the corrosion current density of C-steel with and without Harmal extract respectively. Also, θ was calculated using the following Equation (4):

$$\theta = 1 - \frac{icorr(i)}{icorr(0)} \tag{4}$$

3. Results and Discussion

3.1. FT-IR and UV-Visible Spectroscopy of Harmal Extract

3.1.1. FTIR Spectra

Figure 1 shows the chemical structures of the major constituents of the tested Peganum Harmala extract [38]. The structures contain various electron-rich functional groups such as amine, imine fused pyrrole, hydroxyl, ether and aryl groups. These constituents with functional groups containing oxygen and nitrogen atoms can donate lone pair electrons and bind to the metal ions. Therefore, they can be particularly useful as inhibitors for metal corrosion [46]. FTIR analysis of dried Harmal leaves and extract was undertaken to further confirm the presence of these groups in the materials, Figure 2a. The stretching bands at 3294.12 cm^{-1} is due to O-H and N-H stretch, while the bands at 2939.01 and 2832.78 cm^{-1} are related to the C-H stretching frequency. The broad medium band centered at around 1593.44 cm^{-1} is related to C=N stretch and aromatic rings C=C stretch. It is shifted to lower wavenumbers in the extract compared to the dried Harmal leaves. The C-N stretch and C-O stretch can be assigned to the strong peak at 1017.56 cm^{-1}. The FT-IR results indicated that the Harmal extract contains nitrogen and oxygen functional groups that can act as adsorption centers on the surface of iron steel. Comparison of the FTIR results of dried Harmal and its extract indicates that the extraction method is effective.
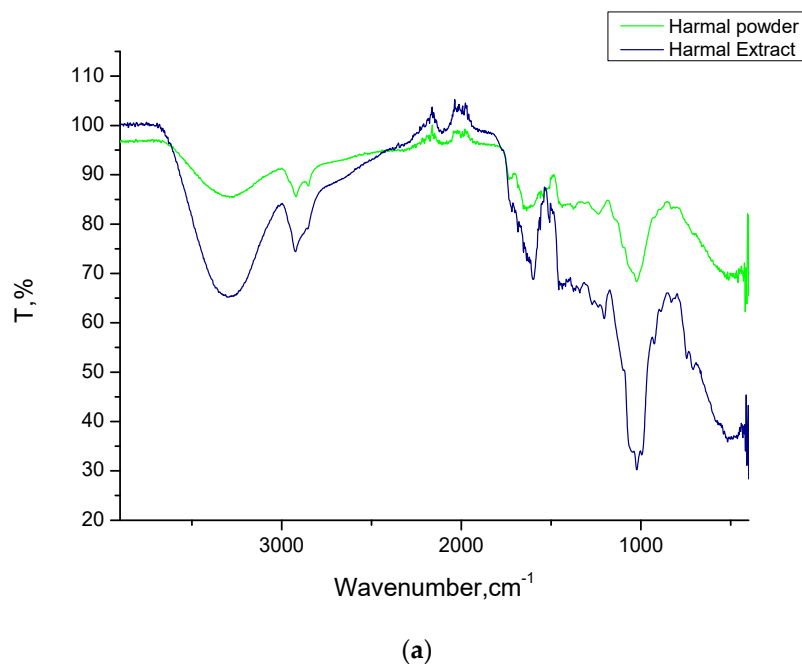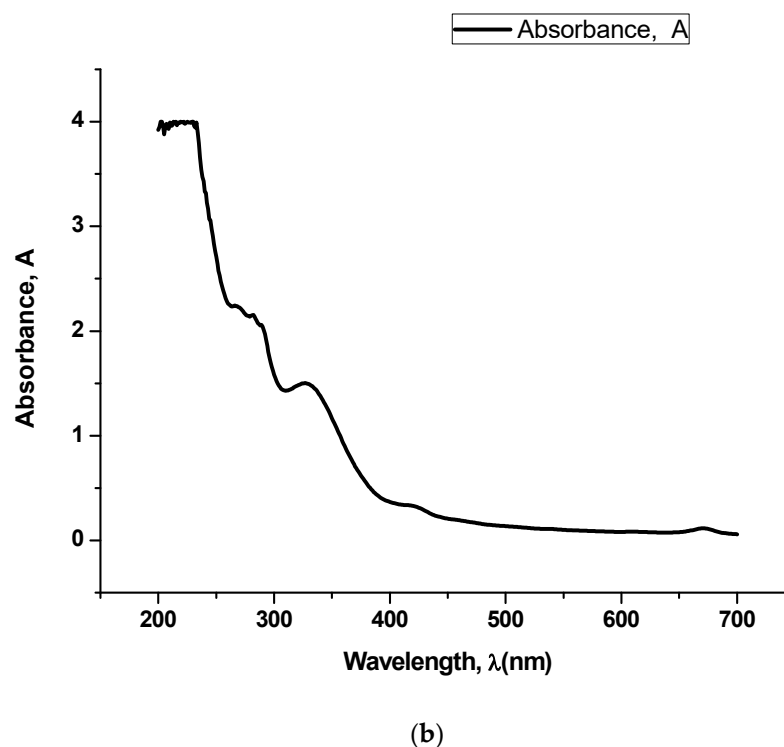

(**a**)

Figure 2. *Cont.*

(**b**)

Figure 2. (**a**) FTIR spectra of Harmal leaves before and after extraction. (**b**) UV-visible spectra of Harmal extract aqueous solution.

3.1.2. UV-Visible Spectra

In the UV-Vis spectra the presence of one or more peaks in the 200 to 400 nm region is an indication of the presence of unsaturated groups and functional groups with heteroatoms such as sulfur, nitrogen, and oxygen. Figure 2b shows UV-Vis the spectrum for Harmal extract. Peak at the positions 334 nm reveals the presence of alkaloids, [47]. These results are in agreement with the FTIR results.

It is out of the scope of the present work to identify the individual species present in the extract of Harmal leaves. But one can refer to Fahmy et al. work. Where, ultraperformance liquid chromatography−electrospray ionization−tandem mass spectrometry (UPLC/ESI-MS) and reversed-phase high-performance liquid chromatography (RP-HPLC) were used to identify 15 alkaloids present in Harmal seed extracts, like harmine, harmol, etc. [39].

3.2. Electrochemical Impedance Spectroscopy Measurements (EIS)

The open-circuit potential, E_{OCP} was applied 15 min before electrochemical impedance study (EIS) experiments. This method studies the amount of current flow and the value of resistance in presence and absence of the Harmal extract. Stable values of E_{OCP} of C-steel were achieved after 900 s for all samples in 0.25 M H_2SO_4 medium with and without the addition of Harmal extract. The obtained results are shown in Figure 3. The E_{OCP} values are shifted in the negative direction as the Harmal extract is added. This behavior is related to the adsorption of inhibitor molecules on active sites on the surface of C-steel [48–50].
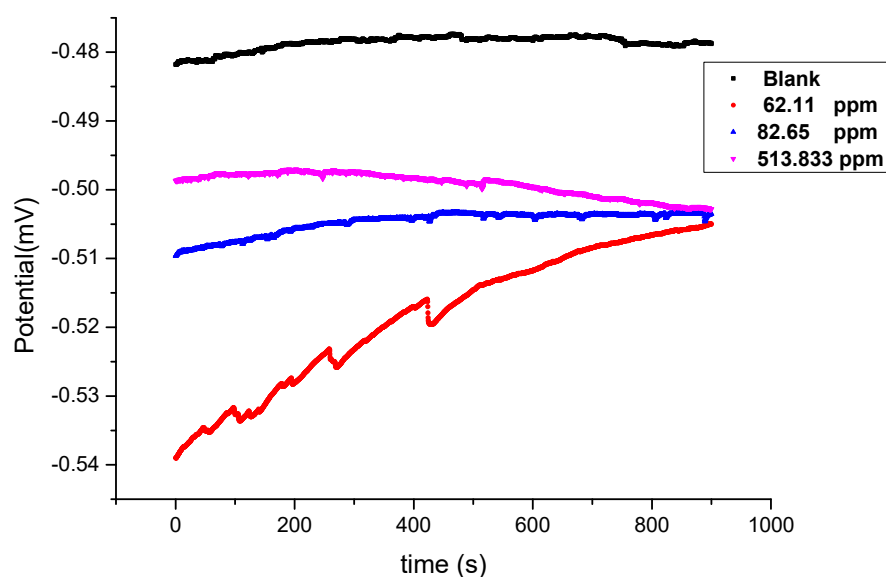
Figure 3. The open circuit potential E_{OCP} plot versus time (s) of C-steel with and without the addition of Harmal extract in 0.25 M H_2SO_4 medium.

All measurements of electrochemical impedance were fitted against equivalent electrical circuit (EEC) models A, B and C that were shown in Figure 4a–c. The Nyquist plots (Figures 5–7) show that the presence of Harmal extract does not change the impedance diagram "semicircle". This behavior indicates that the charge transfer process mainly controls the corrosion of C-steel. It is also noted that the addition of the Harmal extract leads to an increase in the diameter of the Nyquist plot with an increase in the inhibitor concentration. This can be due to the increase in the number of adsorbed Harmal molecules on the surface of C-steel with increasing Harmal extract concentration. In general, a deviation from a semicircle indicates some heterogeneity or roughness of the surface of the C-steel [51].

The EEC model A with only one time constant (The Randle's CPE equivalent circuit) is used in order to fit the impedance data, Figure 5. The obtained electrochemical parameters with the protection efficiency are recorded in Table 1. The resistance of electrolyte (R_s) is shorted by a constant phase element (CPE) that is in parallel to the charge transfer resistance (R_{ct}). (R_s) describes the ohmic resistance while (R_{ct}) represents the inhibitor's resistance towards oxidation of the metal surface by retarding the electrolytes reaching the coating/metal interface, and it is inversely proportional to the corrosion rate [52]. Pure double layer capacitor (C_{dl}) is replaced by a constant phase element (CPE) to provide a more precise fit of the Nyquist plot [53]. The Nyquist plot reveals that increasing the concentration of inhibitor causes an increase in both the diameter of the semicircles and the Rct values, hence an increase in the corrosion inhibition efficiency. From the ohmic law where $V = iR$, the higher the resistance value (R_{ct}), the lower the electrical current (i) flow, the lower the number of electrons transferred across the metal surface. Thus, oxidation of iron is inhibited [52,54]. However, the impedance data at high inhibitor concentration was not well fitted by Randle's CPE equivalent circuit, where the fitting curve is not in agreement with the experimental data in the intermediate and low frequencies.

The surface coverage θ increases from 0.340 at 20.79 ppm of extract to 0.912 at the optimum concentration 283.4 ppm. At low inhibitor concentration the inhibitor is selective and bind specifically to active surface sites that would be most vulnerable to corrosion initiation. But as the inhibitor concentration increases to an optimum value, a protective layer form with more coverage area is achieved. Further increase in concentration does not improve inhibition beyond the optimum value.

Thus, equivalent electrical circuit model B with two time constants was used, (Figure 6). It gave a better fitting of impedance data for all range of concentration including the blank solution, Table 2. In general, each electrochemical process in the circuit should be rep-

resented by a separate distinct semicircle in the Nyquist plot. But when their capacitive nature has short time to relax during the change in the boundary conditions, overlapped arcs are observed in the EIS. Also, due to the high frequency limit, the first semicircle is difficult to see [6,55,56]. This result indicates that the simple prediction of the number of the time constant of the impedance spectrum from the number of capacitive loops in Nyquist plots is inadequate [57]. The fitted model B consists of two circuits connected in series and contains solution resistance (R_s), film resistance (R_f), charge-transfer resistance (R_{ct}), constant phase element of the film (CPE_f) and of the double layer (CPE_{dl}). The double layer capacitance (C_{dl}) can be also calculated from the values of R_{ct}, the impedance of CPE_{dl} (Z_{CPE}), and the exponents of CPE_{dl} (n) [58]. R_f or coating resistance (R_c) is often used for an intact film/coat which act as an isolation layer and provide a good protective performance [59].
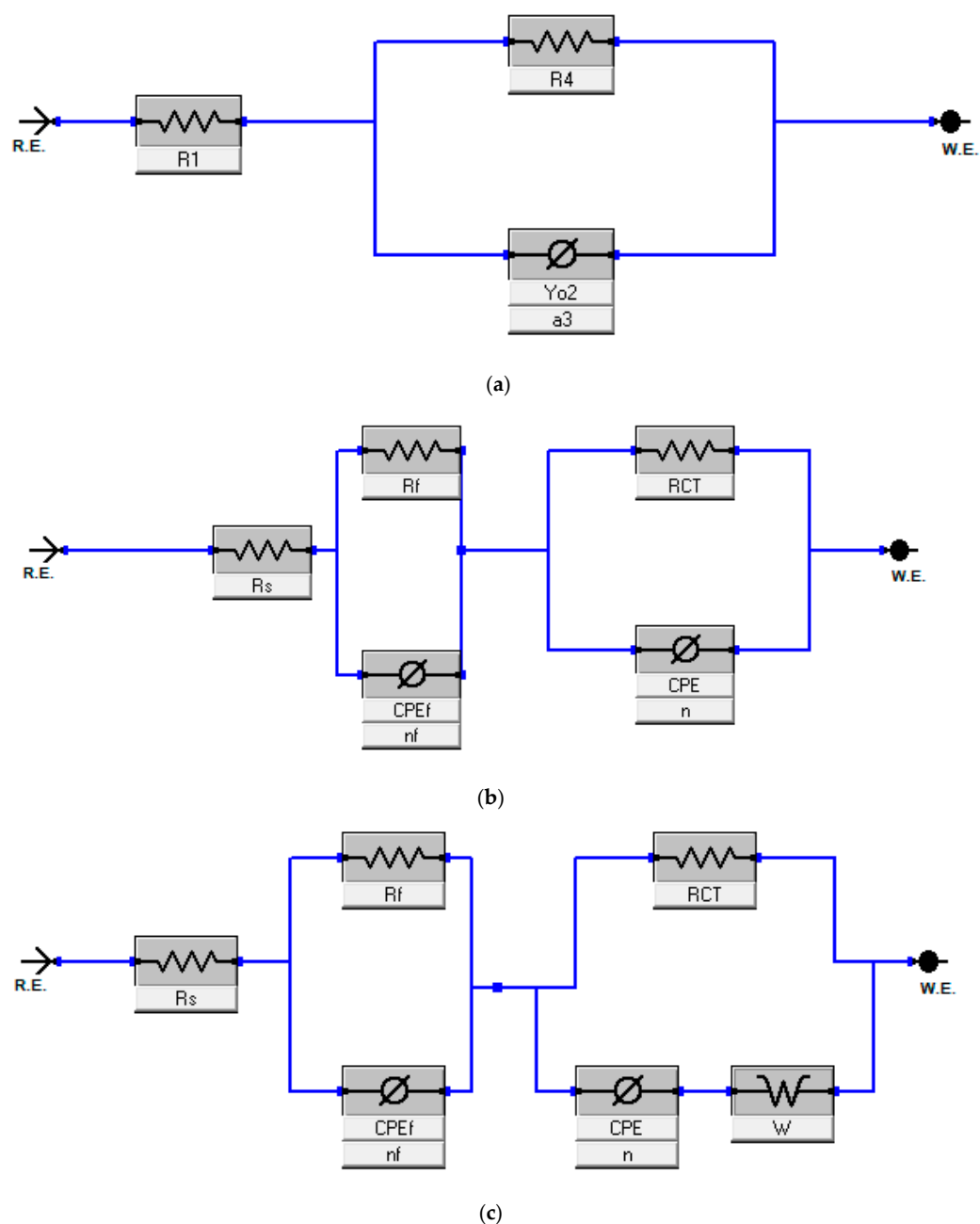

(**a**)

(**b**)

(**c**)

Figure 4. The electrical equivalent circuit (EEC) used to fit the impedance plots data (**a**–**c**) for models A, B and C respectively. (**a**) Model A. (**b**) Model B. (**c**) Model C.

Figure 5. Nyquist plots in 0.25 M H_2SO_4, fitted by equivalent circuit model A for all concentrations of Harmal extract (0, 20.79, 41.49, 62.11, 82.65, 204.1, 283.4, 625.0 and 826.5 ppm).

Figure 6. Nyquist plots in 0.25 M H_2SO_4, fitted by equivalent circuit model B for all concentrations of Harmal extract (0, 20.79, 41.49, 62.11, 82.65, 204.1, 283.4, 625.0 and 826.5 ppm).
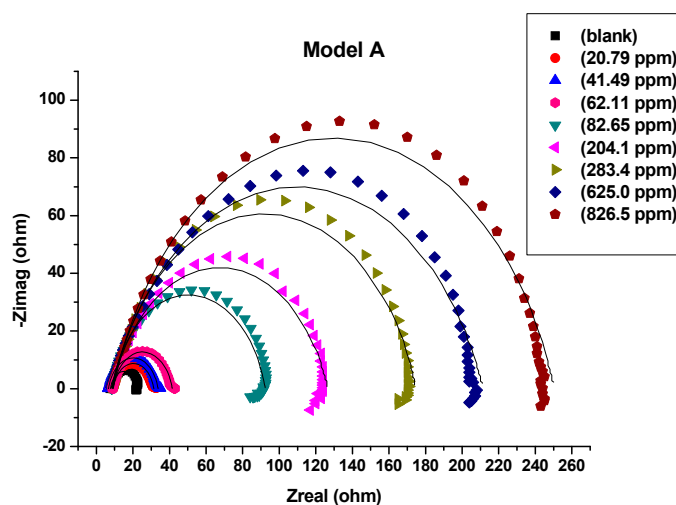

Figure 7. Nyquist plots in 0.25 M H_2SO_4, fitted by equivalent circuit model C for all concentrations of Harmal extract (0, 20.79, 41.49, 62.11, 82.65, 204.1, 283.4, 625.0 and 826.5 ppm).
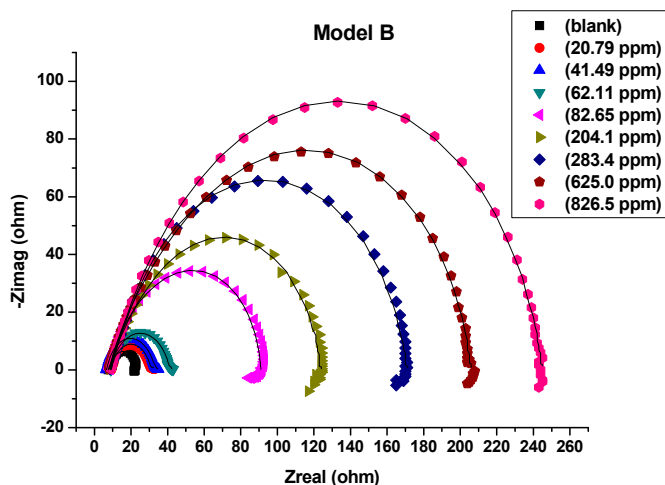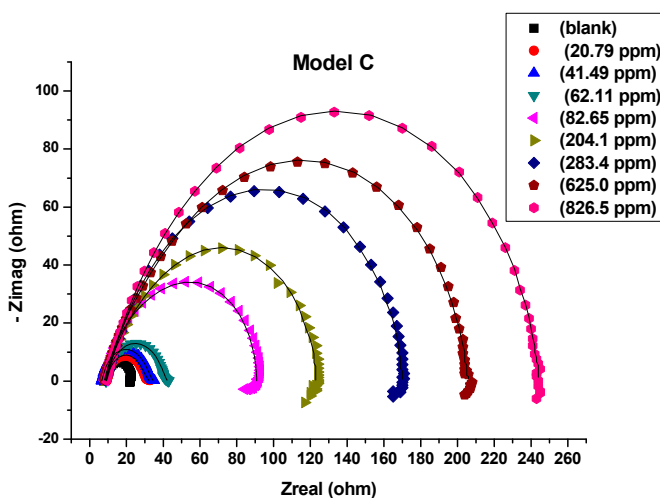
Table 1. Impedance parameters for Harmal extract on C-steel in 0.25 M H_2SO_4 medium by fitting the equivalent circuit model A.

Harmal Extract ppm	R_S Ω cm^2	R_{ct} Ω cm^2	Z_{CPE} $\mu\Omega^{-1}$ s^n cm^{-2}	n	C_{dl} μF/cm^2	θ	IE%
0	15.43	7.37 ± 1	519.2	0.877	238.6	-	-
20.79	18.26	11.18 ± 2	396.5	0.851	153.5	0.340	34.0
41.49	13.18	13.63 ± 2	356.9	0.852	141.6	0.459	45.9
62.11	17.88	16.37 ± 2	328.0	0.846	126.6	0.549	54.9
82.65	16.87	42.16 ± 4	144.3	0.840	54.74	0.825	82.5
204.1	16.90	59.32 ± 5	164.5	0.788	47.32	0.876	87.6
283.4	17.54	83.40 ± 7	148.2	0.804	50.77	0.912	91.2
625.0	15.98	102.25 ± 10	134.4	0.768	36.74	0.928	92.8
826.5	18.14	121.20 ± 13	118.8	0.796	40.00	0.939	93.9

Table 2. Impedance parameters for Harmal extract on C-steel in 0.25 M H_2SO_4 medium by fitting the equivalent circuit model B.

Harmal Extract ppm	R_S Ω cm^2	R_f Ω cm^2	Z_{CPEf} $\mu\Omega^{-1}$s^n cm^{-2}	n_f	R_{ct} Ω cm^2	Z_{CPE} $\mu\Omega^{-1}$s^n cm^{-2}	n	$R_f + R_{ct}$	C_{dl} μF/cm^2	θ	IE%
0	3.83	5.98	359.06	1.00	1.37 ± 1	1150.79	0.800	7.35	229.01	-	-
20.79	4.29	10.00	292.22	0.906	-	-	0.145	-	-	-	-
41.49	3.21	3.10	49,090	0.409	11.31 ± 2	248.46	0.926	14.41	155.36	0.879	87.9
62.11	4.53	16.11	311.12	0.853	0.68 ± 1	-	1.00	16.78	-	-	-
82.65	4.23	15.81	274.72	0.795	25.71 ± 3	122.50	0.996	41.52	120.35	0.947	94.7
204.1	4.16	14.00	460.91	0.708	44.03 ± 4	108.33	0.937	58.03	76.15	0.969	96.9
283.4	4.21	7.96	1269.35	0.625	73.70 ± 8	98.33	0.904	81.65	58.58	0.981	98.1
625.0	4.00	23.94	268.35	0.727	75.61 ± 7	96.16	0.915	99.54	60.87	0.982	98.2
826.5	4.48	29.27	418.94	0.704	89.38 ± 9	94.89	0.916	118.65	61.27	0.985	98.5

The fitting of electrochemical data of different Harmal extract concentrations are exhibited in Table 2. The polarization resistance R_p ($R_p = R_{ct} + R_f$) values always keeps higher with increasing concentrations of Harmal extract, which means that it can provide effective corrosion inhibition. It reveals that increasing the concentration results in a more compact passivation film to isolate the iron from dissolution by sulfuric acid ions [58,60].

EEC model C was applied, which added a diffusion component to model B to fit the experimental data, (Figure 7). If the diffusion region is next to the inhibitor film/metal interface, the mass transfer of reactive species is delayed, resulting in a diffusion characteristic of EIS, like Warburg impedance *W* [59]. The results of fitting the data to model C is presented in Table 3. Unlike the result of fitting of model B, the % efficiency of corrosion inhibition increases smoothly from 60 to 93% for the increase of Harmal extract concentration from 82.65 ppm to 826.5 ppm.

The increase in R_{ct} and decrease in CPE impedance values upon addition of Harmal extract indicated reduction in the corrosion rate with increase in electrical double layer thickness due to the formation of adsorbed protective film on the metal-solution interface. The inhibition action suppresses both the impedance Z_{CPE} and corrosion current density (i_{corr}) due to replacement of water molecules present on the surface of steel electrode surface by the inhibitor ones [52], Tables 1–3.

The increase in the n value (0.905–0.997) in the case of inhibited system, compared to the n value obtained in the blank aggressive medium (0.800), could be attributed to a lessening of surface heterogeneities, Table 2 [60]. Moreover, a significant decrease in the

electrical double layer capacitance Cdl values with increase in inhibitor concentration can be due to the development of a defensive film on the metal interface. The values of Cdl decrease from 229.0 $\mu F/cm^2$ for the C-steel in the blank to 58.6 $\mu F/cm^2$ for the optimum concentration of Harmal extract 283.4 ppm, then it remains almost constant, model B (Table 2). Meanwhile the values of C_{dl} decreases smoothly from 238.6 $\mu F/cm^2$ for the blank to 36.74 $\mu F/cm^2$ for the solution with 625.0 ppm Harmal extract, using model A fitting, Table 1.

Table 3. Impedance parameters for Harmal extract on C-steel in 0.25 M H_2SO_4 medium by fitting the equivalent circuit Model C.

Harmal Extract ppm	R_S Ω cm^2	R_f Ω cm^2	Z_{CPEf} $\mu\Omega^{-1}s^n$ cm^{-2}	n_f	R_{ct} Ω cm^2	Z_{CPE} $\mu\Omega^{-1}s^n$ cm^{-2}	n	W mS s$^{1/2}$	C_{dl} $\mu F/cm^2$	θ	IE%
0	3.78	0.60	4207.3	1.00	6.82 ± 1	308.7	1.00	11.47	308.73	-	-
20.79	4.51	7.83	221.2	0.975	3.97 ± 1	-	0.358	8.858	-	-	-
41.49	3.24	10.38	234.3	0.946	3.80 ± 1	-	0.999	9.442	-	-	-
62.11	4.41	13.01	236.9	0.924	3.87 ± 1	-	0.969	8.784	-	-	-
82.65	4.11	24.63	140.0	1.00	16.91 ± 2	113.0	0.931	4.915	71.08	0.597	59.7
204.1	4.07	40.15	115.0	0.957	17.80 ± 2	214.8	0.828	3.623	67.59	0.617	61.7
283.4	4.09	58.11	115.4	0.944	23.27 ± 3	194.4	0.907	2.310	111.74	0.707	70.7
625.0	3.94	12.59	226.0	0.786	86.87 ± 8	82.6	0.916	4.479	52.52	0.922	92.2
826.5	4.44	24.76	389.3	0.731	93.75 ± 9	89.2	0.925	7.970	60.53	0.927	92.7

The decrease in Cdl can result from a decrease in local dielectric constant and/or an increase in the thickness of the electrical double layer, suggesting that inhibition by molecules can be assisted by their adsorption at the metal/solution interface due to increase in surface coverage (θ) [6,61]. The highest protection capacity values 98% occurred with 283.4 ppm the optimum concentration of added Harmal extract, Table 2.

Bode and Bode phase plots: log (imaginary part of impedance) (log $|Z|$ (ohm)), and phase angle (°) were plotted against log frequency (log*f* (Hz)), Figure 8a,b respectively, for C-steel in 0.25 M H_2SO_4 in the absence and presence of Harmal extract.

The α value indicates the alloy surface irregularity. It is calculated from the slope of the linear region of log(f) versus log$|Z|$ plots (Figure 8a). The α values for C-steel in 0.25 M H_2SO_4 (with and without Harmal extract) were calculated. Ideally, the value of α should be equal to −1 for an ideal capacitor. Coarseness and heterogeneity of the C-steel surface was attained for less than −1 values. It can be seen that the presence of Harmal extract increased the α value to more negative values from −0.256, −0.279, −0.366, −0.347, −0.489, −0.499, −0.562, −0.543, to −0.587 for concentration of Harmal extract ranging from 0, 20.79, 41.49, 62.11, 82.65, 204.1, 283.4, 625.0, to 826.5 ppm. The decrease of heterogeneity of C-steel surface occurred as a result of adsorption of Harmal extract [61].

Figure 8b shows phase angle (°) plotted against (log f (Hz)). It is clear that increasing Harmal extract causes more negative values of phase angle at the intermediate frequency; the phase angle values were −24.15° (0 ppm), −32.43° (62.11 ppm), −44.44° (82.65 ppm), −44.93° (204.1 ppm), −49.89° (283.4 ppm), −48.91° (625 ppm), and −51.88° (826.5 ppm). As the concentration of Harmal extract increases, the values of phase angle become more negative. This indicates that the inhibitive behavior occurred because more of the Harmal molecules adsorbed at the C-steel surface [61].
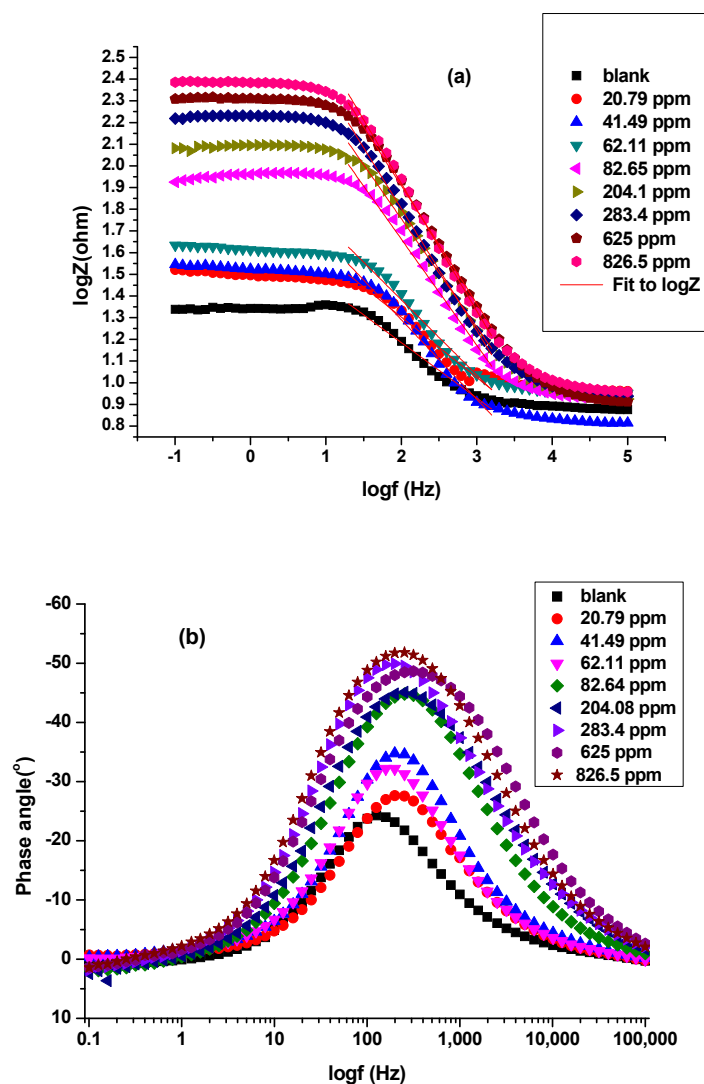
Figure 8. Bode (**a**) and Bode phase (**b**) plots of a C-steel electrode in 0.25 M H$_2$SO$_4$ solution with and without different concentrations of Harmal extract. The α values were calculated from the slopes (red lines) of Bode plots.

3.3. Polarization Curve Measurements

The polarization curves for the corrosion of C-steel in 0.25 M H$_2$SO$_4$ in the presence and absence of Harmal extract were shown in Figure 9. The Tafel plots indicate that the addition of Harmal extract does change potential E_{corr} significantly, noting that the current density i_{corr} decreases, this is due to the inhibitory effect of the Harmal extract, Table 4. Furthermore, increasing the Harmal extract from 62.11 ppm to 826.5 ppm leads to alter cathodic Tafel slope βc (mV dec^{-1}) much more than the anodic Tafel slope βa (mV dec^{-1}) values. This indicates that more inhibition effect of Harmal extract occurs on the cathodic process than on the anodic process Table 4, [61].

Table 4 shows that the addition of the Harmal extract leads to a significant decrease in the corrosion current i_{corr} as it decreases from 12.70 mA/cm^2 to 6.02 mA/cm^2 in the absence and presence of 513.83 ppm of Harmal extract respectively. The corrosion potential E_{corr} shifts in a random way to more negative values with increasing Harmal extract concentration due to an increase in inhibition. Moreover, it is clear that a high IE% 50.2% was attained at 283.4 ppm of Harmal Extract, then it remains almost constant for further increase in concentration. This suggests that the Harmal extract has a moderate inhibition of C-steel corrosion based on polarization studies. Since the shift in Ecorr towards anode or cathode of inhibitor solutions with reference to blank solution is equal to 170 mV (greater

than 85 mV), then the inhibitor is not a mixed inhibitor. It can be classified as a cathodic-type inhibitor [51].
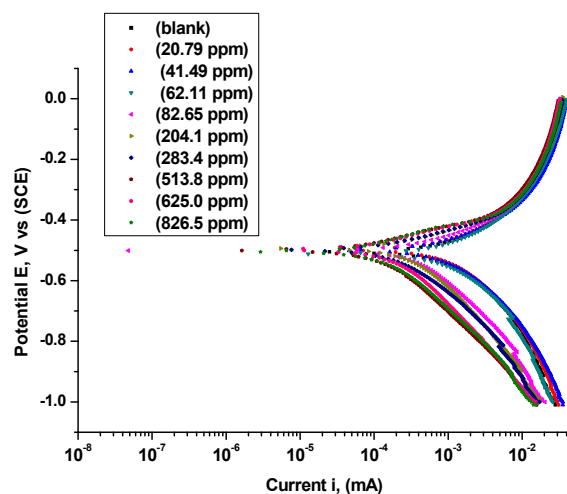

Figure 9. Tafel plots for C-steel in 0.25 M H_2SO_4 containing different concentrations of Harmal extract (0, 20.79, 41.49, 62.11, 82.65, 204.1, 283.4, 625.0 and 826.5 ppm).

Table 4. Polarization parameters for Harmal extract on C-steel in 0.25 M H_2SO_4 medium.

Harmal Extract ppm	i_{cor} mA cm^{-2}	E_{cor} (V) vs. SCE	β_c mV dec^{-1}	β_a mV dec^{-1}	θ	IE%
0	12.70	−642.9	−580.9	794.4	0.000	0.0
20.79	12.60	−583.3	−610.5	712.8	0.008	0.8
41.19	12.41	−607.1	−474.1	690.7	0.023	2.3
62.11	10.00	−666.7	−480.7	705.1	0.213	21.3
82.65	9.06	−761.9	−423.1	808.1	0.286	28.6
204.10	8.12	−785.7	−390.8	791.1	0.361	36.1
283.40	6.32	−738.0	−364.1	680.2	0.502	50.2
513.83	6.02	−785.7	−294.1	758.1	0.526	52.6
625.00	6.65	−812.5	−309.7	791.8	0.477	47.7
826.50	6.45	−785.7	−340.9	748.5	0.493	49.3

There is a difference between the results of inhibition in EIS and potentiodynamic polarization techniques. Tafel analysis is based on current measurement in the time domain while electrochemical impedance in the frequency domain. Also, Tafel analysis is based on dc measurement, while EIS is on an ac one. A study has been performed to find how those two techniques can be correlated with less discrepancy between them, [62]. Here, the Tafel slopes (Tafel constants) are not well as values compared to the one obtained by impedance spectroscopy, particularly for less ideal Tafel plots like the ones we obtained. Thus, we adopt the θ values obtained from impedance techniques.

3.4. Comparison of IE%

The inhibition efficiency of Harmal leaves extract in sulfuric acid media was compared with those of three other plant extracts reported in the literature, Table 5. The results showed that Harmal extract is more effective toward inhibition of C-steel corrosion compared to leaves extract of Psidium Guajava, Tephrosia purpurea and Aegle marmelos, [22,63,64]. IE% for 204.1 ppm Harmal extract was 96.9%, while it was for 200 ppm extract of each of

Psidium Guajava (49%), Tephrosia purpurea (89.4%), and Aegle marmelos (72.21%). Thus, Harmal extract was the most efficient inhibitor among the compared samples.

Table 5. Percent inhibition efficiency (IE%) toward C-steel corrosion by extract of Harmal, Psidium Guajava, Tephrosia purpurea and Aegle marmelos leaves at various concentration C (ppm).

C_{Harmal} (ppm) This Work	IE%	$C_{Psidium\ Guajava}$ (ppm) [22]	IE%	$C_{Tephrosia\ purpurea}$ (ppm) [63]	IE%	$C_{Aegle\ marmelos}$ (ppm) [64]	IE%
0	-	0	-	0		0	
20.79	-	20	15	50	56.3	100	68.05
41.49	87.9	50	21	100	65.2	200	72.21
62.11	-	200	49	150	77.7	300	74.45
82.65	94.7	400	80	200	89.4	400	76.69
204.1	96.9	800	82	250	91.3	500	81.85
283.4	98.1	1200	82	300	92.5	-	-
625.0	98.2	-	-	350	91.1	-	-
826.5	98.5	-	-	400	90.9	-	-

3.5. Inhibition Mechanism and Adsorption Isotherm

It is well established that the effect of the inhibitor on the corrosion rate is related to the adsorption of the anticorrosion molecules on the surface of the metal. The inhibition occurred by two mechanisms [65].

The first mechanism is geometric blocking, which depends on reduction reducing the surface area exposed to corrosion by adsorption of the anti-corrosion molecules. The second mechanism includes energy changing of the cathodic or anode reaction, which is called the energy effect. There is no procedure that can be used to specify which of the mechanisms is responsible for these processes. Theoretically, there is no change in the corrosion potential if the geometric blocking is stronger than the energy effect [66].

The inhibition effect can be explained by adsorption of Harmal extract at the C-steel surface. The Harmal extract replaces the water molecules at the metal interface according to the following Equation (5) [67,68]:

$$\text{Harmal (sol)} + n\text{H}_2\text{O(ads)} \rightarrow \text{Harmal (ads)} + n\text{H}_2\text{O(sol)} \tag{5}$$

For the fitting, the Langmuir adsorption model was applied. Plotting the experimental data C/θ versus C resulted in a fitted straight line as shown in Figure 10a. C (ppm) is the inhibition concentration of Harmal extract and θ is the surface coverage. It is clear that the adsorption follows Langmuir adsorption isotherm, as indicated by the adjusted correlation coefficient = 1.0 and the slope = 1.010 as expected from Langmuir model Equation (6) [61]:

$$c/\theta = c + 1/K_{ads} \tag{6}$$

Thus, the adsorption of Harmal extract as corrosion inhibitor was harmonious with Langmuir adsorption isotherm. The strength and stability of the adsorbed layer formed by Harmal extract was evaluated from inverse of the plot intercept. The K_{ads} was found to be equal to 0.239 (ppm^{-1}).

The fitting of Temkin model was achieved by plotting $\log(\theta/C)$ versus θ, Figure 10b. The obtained straight line has adjustable correlation coefficient R = 0.742. Thus, Temkin model is less acceptable than Langmuir model because of less R value [52].

The plot of Freumkin model, $\log(\theta/(1-\theta)C)$ versus θ gave a large error and almost zero R value, Figure 10c. Thus, this model is not suitable to explain adsorption of Harmal extract onto C-steel [52].

3.6. Surface Analysis

SEM analysis was used to study microscopic surface morphology of pristine C-steel (Figure 11a) and C-steel immersed in H_2SO_4 solution (0.25 M) for 3 h without and with Har-

mal extract addition, Figure 11b,c respectively. The morphology in Figure 11b shows that the surface of C-steel without Harmal extract is rough and highly corroded. However, in the presence of 332 ppm Harmal extract (Figure 11c), the corrosion activity was suppressed, and a slightly smooth surface was observed. This can be related to the adsorption of Harmal extract on C-steel surface, which forms a monolayer of protection against corrosion activity [69].
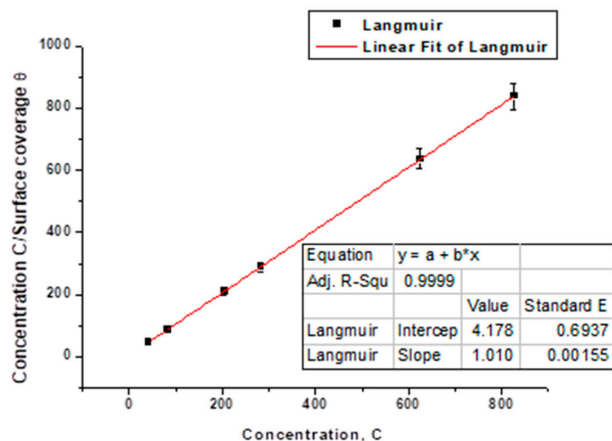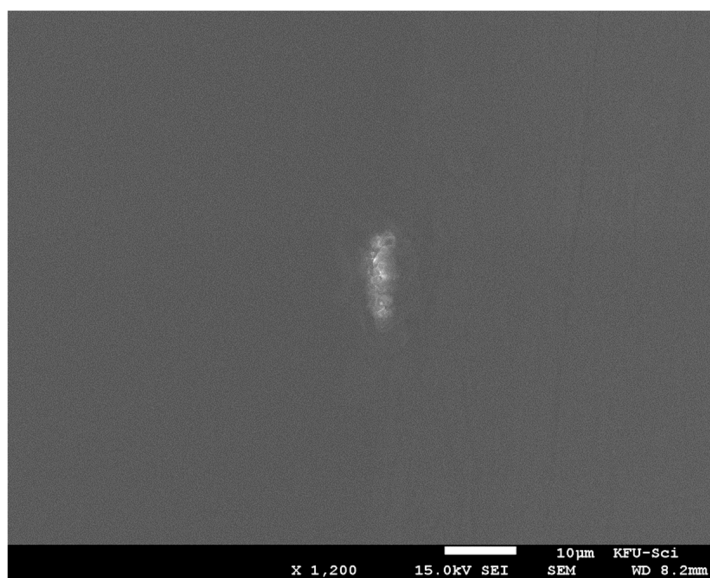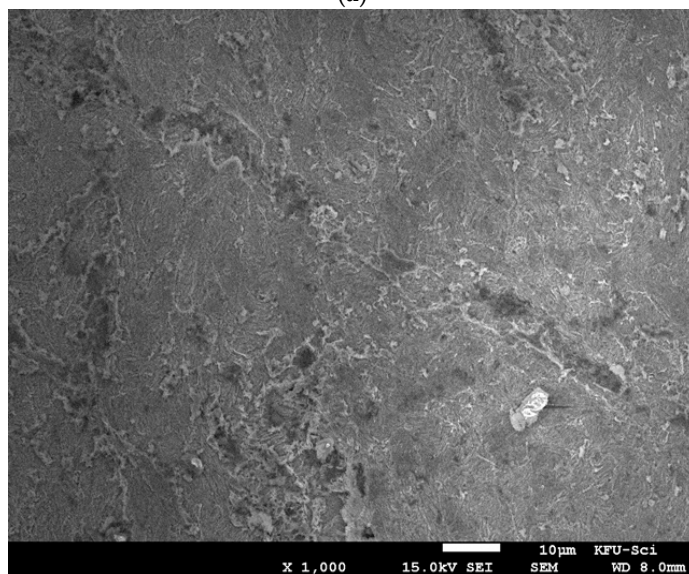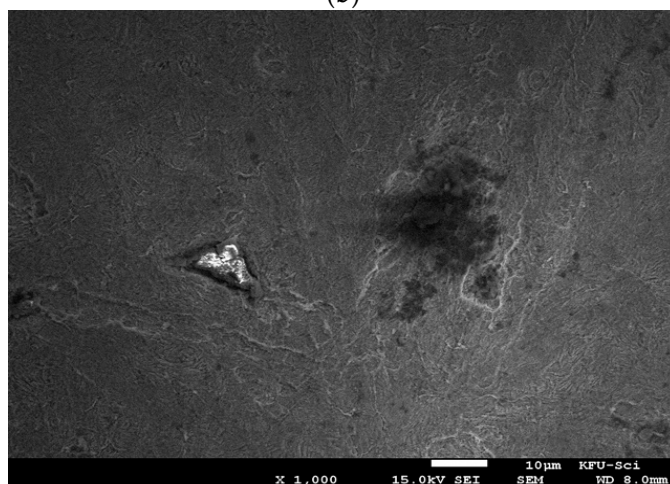

(**a**)
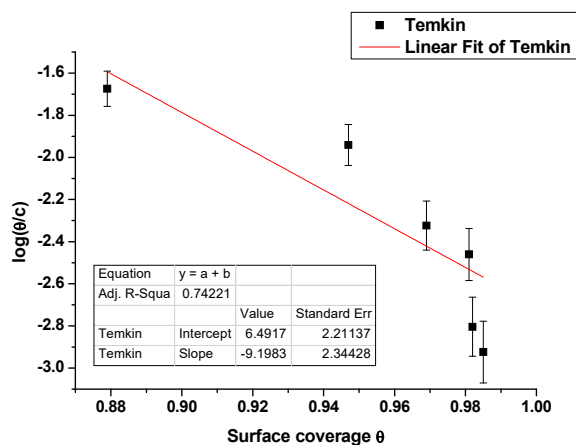
(**b**)
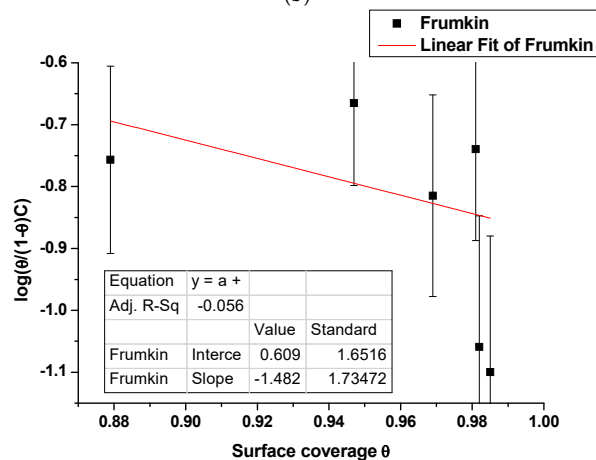
(**c**)

Figure 10. Adsorption isotherm from EIS plots for Harmal extract concentrations (ppm) on C-steel in 0.25 M H_2SO_4 medium: (**a**) Langmuir model, (**b**) Temkin model, and (**c**) Frumkin model.

(**a**)

(**b**)

(**c**)

Figure 11. SEM micrographs for pristine C-steel (**a**) and C-steel immersed in 0.025 M H_2SO_4 for 3 h: corroded C-steel (**b**) and inhibited C-steel by addition of Harmal extract (332 ppm) (**c**).

4. Conclusions

In this work, the efficacy of Harmal extract as an environmentally friendly inhibitor was demonstrated by investigating the electrochemical behavior of C-steel in solutions of 0.25 M H_2SO_4. The polarization curves indicate that Harmal extract acts as a cathodic-type inhibitor. It was also observed from the impedance plots that the charge transfer process mainly controls the corrosion of C-steel. The electrical double layer capacitance values C_{dl} decreases while the charge transfer resistance R_{ct} increases with increase in Harmal extract concentration, indicating the formation of protective film. Moreover, Harmal extract demonstrates high efficacy of 98% using electrochemical impedance spectroscopy measurements at the optimum concentration 283.4 ppm. This indicates a high sensitivity of Harmal extract toward inhibition of C-steel in acidic medium. It was also observed that adsorption follows Langmuir isotherm. The electron-rich functional groups in the constituent of Harmal extract that contribute to anticorrosion, were determined by FTIR. SEM measurement of the steel electrode surface clearly demonstrates the inhibition effect of Harmal leaves.

Author Contributions: Conceptualization, H.H.H. and N.A.O.; methodology, N.A.O. and H.H.H.; software, N.A.O. and H.H.H.; validation, H.H.H.; formal analysis, N.A.O. and H.H.H.; investigation, N.A.O. and H.H.H.; resources, N.A.O. and H.H.H.; data curation, H.H.H.; writing—original draft preparation, N.A.O.; writing—review and editing, H.H.H.; visualization, N.A.O. and H.H.H.; supervision, N.A.O. and H.H.H.; project administration, N.A.O.; funding acquisition, N.A.O. All authors have read and agreed to the published version of the manuscript.

Conflicts of Interest: The authors declare no conflict of interest.

Sample Availability: Samples of the compounds are available from the authors.

References

1. Bardal, E. *Engineering Materials and Processes*; Springer: London, UK; Berlin/Heidelerg, Germany, 2004; pp. 5–10.
2. Koch, G.H.; Brongers, M.P.H.; Thompson, N.G.; Virmani, Y.P.; Payer, J.H. *Corrosion Cost and Preventive Strategies in the United States*; Federal Highway Administration: Washington, DC, USA, 2002.
3. Guo, L.; Qi, C.; Zheng, X.; Zhang, R.; Shen, X.; Kaya, S. Toward understanding the adsorption mechanism of large size organic corrosion inhibitors on an Fe (110) surface using the DFTB method. *RSC Adv.* **2017**, *7*, 29042–29050. [CrossRef]
4. Zaferani, S.H.; Sharifi, M.; Zaarei, D.; Shishesaz, M.R. Application of eco-friendly products as corrosion inhibitors for metals in acid pickling processes–A review. *J. Environ. Chem. Eng.* **2013**, *1*, 652–657. [CrossRef]
5. Li, X.; Xie, X.; Deng, S.; Du, G. Two phenylpyrimidine derivatives as new corrosion inhibitors for cold rolled steel in hydrochloric acid solution. *Corros. Sci.* **2014**, *87*, 27–39. [CrossRef]
6. Tabesh, R.N.; Abdel-Gaber, A.M.; Hammud, H.H.; Al-Oweini, R. Inhibition of Steel Corrosion in Sulfuric Acid Solution by 1, 10-Phenanthroline, para-Aminobenzoate and their Corresponding Manganese Complex. *Z. Für Phys. Chem.* **2019**, *233*, 1553–1569. [CrossRef]
7. Verma, C.; Olasunkanmi, L.O.; Ebenso, E.E.; Quraishi, M.A. Substituents effect on corrosion inhibition performance of organic compounds in aggressive ionic solutions: A review. *J. Mol. Liq.* **2018**, *251*, 100–118. [CrossRef]
8. Verma, C.; Ebenso, E.E.; Quraishi, M.A. Corrosion inhibitors for ferrous and non-ferrous metals and alloys in ionic sodium chloride solutions: A review. *J. Mol. Liq.* **2017**, *248*, 927–942. [CrossRef]
9. Singh, P.; Makowska-Janusik, M.; Slovensky, P.; Quraishi, M.A. Nicotinonitriles as green corrosion inhibitors for mild steel in hydrochloric acid: Electrochemical, computational and surface morphological studies. *J. Mol. Liq.* **2016**, *220*, 71–81. [CrossRef]
10. Hinton, B.R.W. Corrosion prevention and control. *Handb. Phys. Chem. Rare Earths* **1995**, *21*, 29–92.
11. El-Tabesh, R.N.; Abdel-Gaber, A.M.; Hammud, H.H.; Oweini, R. Effect of Mixed-Ligands Copper Complex on the Corrosion Inhibition of Carbon Steel in Sulfuric Acid Solution. *J. Bio Tribo Corros.* **2020**, *6*, 29. [CrossRef]
12. Umoren, S.A.; Eduok, U.M. Application of carbohydrate polymers as corrosion inhibitors for metal substrates in different media: A review. *Carbohydr. Polym.* **2016**, *140*, 314–341. [CrossRef] [PubMed]
13. Hu, K.; Zhuang, J.; Zheng, C.; Ma, Z.; Yan, L.; Gu, H.; Zeng, X.; Ding, J. Effect of novel cytosine-l-alanine derivative based corrosion inhibitor on steel surface in acidic solution. *J. Mol. Liq.* **2016**, *222*, 109–117. [CrossRef]

14. Dakhil, R.M.; Gaaz, T.S.; Al-Amiery, A.A.; Kadhum, A.A.H. Inhibitive impacts extract of Citrus aurantium leaves of carbon steel in corrosive media. *Green Chem. Lett. Rev.* **2018**, *11*, 559–566. [CrossRef]

15. Raghavendra, N. Latest Exploration on Natural Corrosion Inhibitors for Industrial Important Metals in Hostile Fluid Environments: A Comprehensive Overview. *J. Bio-Tribo-Corros.* **2019**, *5*, 54. [CrossRef]

16. Ji, G.; Anjum, S.; Sundaram, S.; Prakash, R. Musa paradisica peel extract as green corrosion inhibitor for mild steel in HCl solution. *Corros. Sci.* **2015**, *90*, 107–117. [CrossRef]

17. Nasrollahzadeh, M.; Sajadi, S.M.; Khalaj, M. Green synthesis of copper nanoparticles using aqueous extract of the leaves of Euphorbia esula L and their catalytic activity for ligand-free Ullmann-coupling reaction and reduction of 4-nitrophenol. *RSC Adv.* **2014**, *4*, 47313–47318. [CrossRef]

18. Sharghi, H.; Khalifeh, R.; Doroodmand, M.M. Copper nanoparticles on charcoal for multicomponent catalytic synthesis of 1, 2, 3-Triazole derivatives from benzyl halides or alkyl halides, terminal alkynes and sodium azide in water as a 'Green' solvent. *Adv. Synth. Catal.* **2009**, *351*, 207–218. [CrossRef]

19. Varma, R.S. Greener and sustainable trends in synthesis of organics and nanomaterials. *ACS Sustain. Chem. Eng.* **2016**, *4*, 5866–5878. [CrossRef]

20. Duan, H.; Wang, D.; Li, Y. Green chemistry for nanoparticle synthesis. *Chem. Soc. Rev.* **2015**, *44*, 5778–5792. [CrossRef]

21. Seo, J.; Lee, S.; Elam, M.L.; Johnson, S.A.; Kang, J.; Arjmandi, B.H. Study to find the best extraction solvent for use with guava leaves (Psidium guajava L.) for high antioxidant efficacy. *Food Sci. Nutr.* **2015**, *2*, 174–180. [CrossRef]

22. Victoria, S.N.; Prasad, R.; Manivannan, R. Psidium guajava leaf extract as green corrosion inhibitor for mild steel in phosphoric acid. *Int. J. Electrochem. Sci.* **2015**, *10*, 2220–2238.

23. Chaudhari, H.G.; Vashi, R.T. The study of henna leaves extract as green corrosion inhibitor for mild steel in acetic acid. *J. Fundam. Appl. Sci.* **2016**, *8*, 280–296. [CrossRef]

24. Aribo, S.; Olusegun, S.J.; Ibhadiyi, L.J.; Oyetunji, A.; Folorunso, D.O. Green inhibitors for corrosion protection in acidizing oilfield environment. *J. Assoc. Arab Univ. Basic Appl. Sci.* **2017**, *24*, 34–38. [CrossRef]

25. Verma, C.; Ebenso, E.E.; Bahadur, I.; Quraishi, M.A. An overview on plant extracts as environmental sustainable and green corrosion inhibitors for metals and alloys in aggressive corrosive media. *J. Mol. Liq.* **2018**, *266*, 577–590. [CrossRef]

26. Soltani, N.; Tavakkoli, N.; Khayatkashani, M.; Jalali, M.R.; Mosavizade, A. Green approach to corrosion inhibition of 304 stainless steel in hydrochloric acid solution by the extract of Salvia officinalis leaves. *Corros. Sci.* **2012**, *62*, 122–135. [CrossRef]

27. Anupama, K.K.; Ramya, K.; Joseph, A. Electrochemical and computational aspects of surface interaction and corrosion inhibition of mild steel in hydrochloric acid by Phyllanthus amarus leaf extract (PAE). *J. Mol. Liq.* **2016**, *216*, 146–155. [CrossRef]

28. Faustin, M.; Maciuk, A.; Salvin, P.; Roos, C.; Lebrini, M. Corrosion inhibition of C38 steel by alkaloids extract of Geissospermum laeve in 1 M hydrochloric acid: Electrochemical and phytochemical studies. *Corros. Sci.* **2015**, *92*, 287–300. [CrossRef]

29. Krishnegowda, P.M.; Venkatesha, V.T.; Krishnegowda, P.K.M.; Shivayogiraju, S.B. Acalypha torta leaf extract as green corrosion inhibitor for mild steel in hydrochloric acid solution. *Ind. Eng. Chem. Res.* **2013**, *52*, 722–728. [CrossRef]

30. Mehdipour, M.; Ramezanzadeh, B.; Arman, S.Y. Electrochemical noise investigation of Aloe plant extract as green inhibitor on the corrosion of stainless steel in 1 M H2SO4. *J. Ind. Eng. Chem.* **2015**, *21*, 318–327. [CrossRef]

31. Hassan, K.H.; Khadom, A.A.; Kurshed, N.H. Citrus aurantium leaves extracts as a sustainable corrosion inhibitor of mild steel in sulfuric acid. *S. Afr. J. Chem. Eng.* **2016**, *22*, 1–5. [CrossRef]

32. Singh, A. Cassia tora Leaves Extract as Mild Steel Corrosion Inhibitor in Sulphuric Acid Solution. *Imp. J. Interdiscip. Res.* **2016**, *2*, 698–701.

33. Sathiyanathan, R.; Maruthamuthu, S.; Selvanayagam, M.; Mohanan, S.; Palaniswamy, N. Corrosion inhibition of mild steel by ethanolic extracts of Ricinus communis leaves. *Indian J. Chem. Technol.* **2005**, *12*, 356–360.

34. Tuaweri, T.J.; Ogbonnaya, E.A.; Onyemaobi, O.O. Corrosion inhibition of heat treated mild steel with neem leave extract in a chloride medium. *Int. J. Res. Eng. Technol.* **2015**, *4*, 2321–7308.

35. Wang, H.; Gao, M.; Guo, Y.; Yang, Y.; Hu, R. A natural extract of tobacco rob as scale and corrosion inhibitor in artificial seawater. *Desalination* **2016**, *398*, 198–207. [CrossRef]

36. Abd-El-Khalek, D.E.; Abdel-Gaberb, A.M. Evaluation of nicotiana leaves extract as corrosion inhibitor for steel in acidic and neutral chloride solutions. *Port. Electrochim. Acta* **2012**, *30*, 247–259. [CrossRef]

37. Anaee, R.A.; Alzuhairi, M.H.; Abdullah, H.A. Corrosion Inhibition of Steel in Petroleum Medium by Ficus Carica Leaves Extract. *Asian J. Eng. Technol.* **2014**, *2*, 2321–2462.

38. Herraiz, T.; González, D.; Ancín-Azpilicueta, C.; Arán, V.J.; Guillén, H. β-Carboline alkaloids in Peganum harmala and inhibition of human monoamine oxidase (MAO). *Food Chem. Toxicol.* **2010**, *48*, 839–845. [CrossRef] [PubMed]

39. Fahmy, S.A.; Issa, M.Y.; Saleh, B.M.; Meselhy, M.R.; Azzazy, H.M.E. Peganum harmala Alkaloids Self-Assembled Supramolecular Nanocapsules with Enhanced Antioxidant and Cytotoxic Activities. *ACS Omega* **2021**, *11*, 11954–11963. [CrossRef]

40. Moloudizargari, M.; Mikaili, P.; Aghaianshakeri, S.; Asghari, M.H.; Shayegh, J. Pharmacological and therapeutic effects of Peganum harmala and its main alkaloids. *Pharmacogn. Rev.* **2013**, *14*, 199–212. [CrossRef]

41. Dao, V.D. An experimental exploration of generating electricity from nature-inspired hierarchical evaporator: The role of electrode materials. *Sci. Total Environ.* **2021**, *759*, 143490. [CrossRef]

42. Dao, V.-D.; Vu, N.H.; Choi, H.-S. All day Limnobium laevigatum inspired nanogenerator self-driven via water evaporation. *J. Power Sources* **2020**, *448*, 227388. [CrossRef]

43. Thomas, K.R.J.; Santos, D. Experimental and DFT studies on the ultrasonic energy-assisted extraction of the phytochemicals of Catharanthus roseus as green corrosion inhibitors for mild steel in NaCl medium. *R. Soc. Chem.* **2020**, *10*, 5399.

44. Hussin, M.H.; Kassim, M.J. The corrosion inhibition and adsorption behavior of Uncaria gambir extract on mild steel in 1 M HCl. *Mater. Chem. Phys.* **2011**, *125*, 461–468. [CrossRef]

45. El Haleem, S.M.A.; El Wanees, S.A.; El Aal, E.E.A.; Farouk, A. Factors affecting the corrosion behaviour of aluminium in acid solutions. I. Nitrogen and/or sulphur-containing organic compounds as corrosion inhibitors for Al in HCl solutions. *Corros. Sci.* **2013**, *68*, 1–13. [CrossRef]

46. Emregul, K.C.; Akay, A.A.; Atakol, O. The corrosion inhibition of steel with Schiff base compounds in 2 M HCl. *Mater. Chem. Phys.* **2005**, *93*, 325–329. [CrossRef]

47. Njokua, D.I.; Chidieberea, M.A.; Oguzieb, K.L.; Ogukwea, C.E.; Oguzie, E.E. Corrosion inhibition of mild steel in hydrochloric acid solution by the leaf extract of *Nicotiana tabacum*. *Adv. Mater. Corros.* **2013**, *1*, 54–61.

48. Radovanović, M.B.; Tasić, Ž.Z.; Mihajlović, M.B.P.; Simonović, A.T.; Antonijević, M.M. Electrochemical and DFT studies of brass corrosion inhibition in 3% NaCl in the presence of environmentally friendly compounds. *Sci. Rep.* **2019**, *9*, 16081. [CrossRef]

49. Badawy, W.A.; Ismail, K.M.; Fathi, A.M. Corrosion control of Cu–Ni alloys in neutral chloride solutions by amino acids. *Electrochim. Acta.* **2006**, *51*, 4182–4189. [CrossRef]

50. Ismail, K.M. Evaluation of cysteine as environmentally friendly corrosion inhibitor for copper in neutral and acidic chloride solutions. *Electrochim. Acta.* **2007**, *52*, 7811–7819. [CrossRef]

51. Bouyanzer, A.; Hammouti, B.; Majidi, L. Pennyroyal oil from Mentha pulegium as corrosion inhibitor for steel in 1 M HCl. *Mater. Lett.* **2006**, *60*, 2840–2843. [CrossRef]

52. Faiz, M.; Zahari, A.A.; Awanga, K.; Hussin, H. Corrosion inhibition on mild steel in 1 M HCl solution by Cryptocarya nigra extracts and three of its constituents (alkaloids). *RSC Adv.* **2020**, *10*, 6547–6562. [CrossRef]

53. Jacob, K.S.; Parameswaran, G. Corrosion inhibition of mild steel in hydrochloric acid solution by Schiff base furoin thiosemicarbazone. *Corros. Sci.* **2010**, *52*, 224–228.

54. Hussin, M.H.; Kassim, M.J.; Razali, N.N.; Dahon, N.H.; Nasshorudin, D. The effect of *Tinospora crispa* extracts as a natural mild steel corrosion inhibitor in 1 M HCl solution. *Arab. J. Chem.* **2016**, *9*, S616–S624. [CrossRef]

55. Liping, S.; Lihua, H.; Hui, Z.; Qiang, L.; Pijolat, C. La substituted Sr2MnO4 as a possible cathode material in SOFC. *J. Power Sources* **2008**, *179*, 96–100. [CrossRef]

56. Haque, J.; Ansari, K.R.; Srivastava, V.; Quraishi, M.A.; Obot, I.B. Pyrimidine derivatives as novel acidizing corrosion inhibitors for N80 steel useful for petroleum industry: A combined experimental and theoretical approach. *J. Ind. Eng. Chem.* **2017**, *49*, 176–188. [CrossRef]

57. Zhang, J.T.; Hu, J.M.; Zhang, J.Q.; Cao, C.N. Studies of impedance models and water transport behaviors of polypropylene coated metals in NaCl solution. *Prog. Org. Coat.* **2004**, *49*, 293–301. [CrossRef]

58. Xue, X.-Z.; Tang, S.; Yue, Y.-B.; Liu, J.-K.; Yang, X.-H. One-step crushing and cladding technology and enhanced anticorrosion activity of Zn3(PO4)2@AlH2P3O10 pigment. *J. Alloy. Compd.* **2018**, *744*, 837–848. [CrossRef]

59. Meng, F.; Liu, L.; Tian, W.; Wu, H.; Li, Y.; Zhang, T.; Wang, F. The influence of the chemically bonded interface between fillers and binder on the failure behaviour of an epoxy coating under marine alternating hydrostatic pressure. *Corros. Sci.* **2015**, *101*, 139–154. [CrossRef]

60. Sayed, A.R.; El-Lateef, H.M.A. Thiocarbohydrazones Based on Adamantane and Ferrocene as Efficient Corrosion Inhibitors for Hydrochloric Acid Pickling of C-Steel. *Coatings* **2020**, *10*, 1068. [CrossRef]

61. Ali, A.I.; Mahrousb, Y.S. Corrosion inhibition of C-steel in acidic media from fruiting bodies of Melia azedarach L extract and a synergistic Ni^{2+} additive. *RSC Adv.* **2017**, *7*, 23687–23698. [CrossRef]

62. Park, K.; Chang, B.-Y.; Hwang, S. Correlation between Tafel Analysis and Electrochemical Impedance Spectroscopy by Prediction of Amperometric Response from EIS. *ACS Omega* **2019**, *4*, 19307–19313. [CrossRef]

63. Karunanithi, B.T.; Chellappa, J. Adsorption and inhibition properties of *Tephrosia Purpurea* as corrosion inhibitor for mild steel in sulphuric acid solution. *J. Dispers. Sci. Technol.* **2019**, *40*, 1441–1450. [CrossRef]

64. Bhardwai, N.; Prasad, D.; Haldhar, R. Study of the *Aegle marmelos* as a Green Corrosion Inhibitor for Mild Steel in Acidic Medium: Experimental and Theoretical Approach. *J. Bio-Tribo-Corros.* **2018**, *4*, 61. [CrossRef]

65. Riggs, O.L., Jr. *Corrosion Inhibitors*; Nathan, C.C., Ed.; NACE: Houston, TX, USA, 1973.

66. Martinez, S.; Metikoš-Huković, M. A nonlinear kinetic model introduced for the corrosion inhibitive properties of some organic inhibitors. *J. Appl. Electrochem.* **2003**, *33*, 1137–1142. [CrossRef]

67. Hosseini, M.; Mertens, S.F.L.; Arshadi, M.R. Synergism and antagonism in mild steel corrosion inhibition by sodium dodecylbenzenesulphonate and hexamethylenetetramine. *Corros. Sci.* **2003**, *45*, 1473–1489. [CrossRef]

68. Rudresh, H.B.; Mayanna, S.M. Adsorption of n-Decylamine on Zinc from Acidic Chloride Solution. *J. Electrochem. Soc.* **1977**, *124*, 340. [CrossRef]

69. Asadi, N.; Ramezanzadeh, M.; Bahlakeh, G.; Ramezanzadeh, B. Utilizing Lemon Balm extract as an effective green corrosion inhibitor for mild steel in 1M HCl solution: A detailed experimental, molecular dynamics, Monte Carlo and quantum mechanics study. *J. Taiwan Inst. Chem. Eng.* **2019**, *95*, 252–272. [CrossRef]